



Augmentation of Nanofluids Heat Transfer in a Circular Tube with Baffled Winged Twisted Swirl Generator

Sami D. Salman*

Ramzi Ata Abd Alsaheb **

*,**Department of Biochemical Engineering/ Al-khwarizmi College of Engineering/ University of Baghdad/ Iraq

*E-mail: sami.albayati@gmail.com

**E-mail: ramzi_eng_1981@yahoo.com

(Received 14 June 2017; accepted 17 July 2017)

<https://doi.org/10.22153/kej.2017.07.006>

Abstract

This article introduces a numerical study on heat exchange and corrosion coefficients of Zinc–water nanofluid stream in a circular tube fitted with swirl generator utilizing CFD emulation. Different forms of swirl generator which have the following properties of plain twisted tape (PTT) and baffle wings twisted tape (BTT) embeds with various ratio of twisting ($\gamma = 2.93, 3.91$ and 4.89), baffle inclination angles ($\beta = 0^\circ, -30^\circ$ and 30°) joined with 1%, 1.5% and 2% volume fraction of ZnO nanofluid were utilized for simulation. The results demonstrated that the heat and friction coefficients conducted by these two forms of vortex generator raised with Reynolds number, twist ratio and baffle inclination angles decreases. Likewise, the results showed that the heat transfer rate raised with accretion of ZnO nanoparticle concentration. Furthermore, the maximum rate of heat transfer with significant intension in friction coefficient has been produced by baffle wings tape with ratio of twisting $\gamma=2.93$ and baffle angle $\beta=-30$ with 2% volume fraction of ZnO nanofluid.

Keywords: Baffled wings twisted tape, Nanofluid, Heat transfer augmentation, Friction factor, Uniform heat flux.

1. Introduction

The thermal performance of heat exchangers can be essentially increased by utilizing heat transfer augmentation techniques. The augmentation techniques can be categorized three major kinds; the active technique, the passive technique and compound technique. The active techniques imposed an extrinsic power like; electrical field, surface vacillation, etc. The passive technique includes additives to gases or liquids, particular face geometries or swirl generator i.e; Tape inserts. However, the combined techniques can be created by utilizing at least two or more active and/or passive techniques. Different exploratory investigations on these augmentation techniques have been conducted using tape inserts [1-10], while

numerical simulation utilizing CFD methods have been reported. Pathipakka G & Sivashanmugam [11] implemented numerical simulation on heat rate characteristics for Al_2O_3 nanofluid with helical inserts in circular tube using FLUENT software version 6.3.2. Various volume fractions (0.5%, 1.0%, 1.5%) of Al_2O_3 nanoparticles in water conjoined helical twist inserts with various ratio of twisting ($\gamma = 2.93, 3.9$ and 4.89) were utilized for numerical simulation. The obtained results have been compared with data collected from literature with great assertion.

Salman et al. [12] have been actualized theoretical study on the heat characteristics and friction factor in circular tube embedded tape with elliptical cut using CFD-FLUENT software version 6.3.26. Two forms of twisted tape have been used; Classical and elliptical cut tapes with

different ratio of twisting ($y=2.93 - 4.89$) and various cut depth ($w = 0.5 - 1.5$ cm) with water as test liquid were utilized for numerical simulation. The results obtained demonstrate that the heat rate and the friction characteristics conducted by twist tape with elliptic cut have been augmented with Reynolds number increasing and decreasing ratio of twisting. Likewise, the result demonstrate that the higher heat transfer rate was obtained by tape of elliptical cut with $w = 0.5$ cm and $y=2.93$.

Salman et al. [13] announced a numerical investigation on heat transfer augmentation in a uniform heat-fluxed tube fitted with V-cut twisted tape in laminar stream of water utilizing FLUENT software. The simulated results demonstrate that the greatest value of heat transfer improvement was acquired by V-cut tape with cut tape with $y=2.93$ $w = 0.5$ cm model. Salman et al. [14] additionally proposed numerical simulation of the heat rate characteristics in a circular tube with twisted tape under steady state heat flux condition using FLUENT software. Plain tapes and baffled tapes with various ratio of twisting ($y = 2.93, 3.91, \text{ and } 4.89$) and various angles of inclination ($\beta= 0^\circ, -30^\circ, \text{ and } 30^\circ$) were used for simulation. The results coordinated with the correlations excerpted from literatures for a plain tube within $\pm 8\%$ and $\pm 7\%$ deviation for Nusselt and friction factors, respectively. Additionally, the results demonstrate that baffled tapes with ratio of twisting $y=2.93$ and inclination angle $\beta= -30^\circ$ produced the greatest heat augmentation.

The present research reports a numerical study for heat transfer improvement in a tube with baffled winged twist tape (BTT) with various ratio of twisting ($y = 2.93, 3.91, \text{ and } 4.89$) and various baffle inclination angle ($\beta= 0^\circ, -30^\circ, \text{ and } 30^\circ$) conjugated with 1%, 1.5% and 2% volume fraction of ZnO nanofluid are accounted. The result acquired offered about 10% improvement for Nusselt number with noteworthy increments in friction characteristics compared with plain twisted tape.

2. Technical Specification

2.1. Baffled Winged Tape Model

Baffled winged twist tape (BTT) model is demonstrated in Figure 1. Aluminium tape of 2.45 cm width and 0.08 cm thickness is consistently twisting over different lengths of 7.5, 10, and 12.5 cm to create different ratio of twisting ($y = 2.93, 3.91 \text{ and } 4.89$). The ratio of twisting 'y' characterized as a fraction of single full twist (360°) length to tape width. Stainless steel tube with diameter of 2.54 cm and length of 180 cm was utilized as test sample, Water and ZnO nanoparticles ($dp=20$ nm) have been chosen as test liquid. The thermo-physical characteristics of substances used for simulation are appeared in Table 1 and Table 2.

Table 1,
Water and ZnO nanofluids Thermo-physical characteristics [15], [16].

Liquid	Density (Kg/m ³)	Specific heat (J/Kg K)	Thermal Conductivity (W/m°C)	Viscosity (N s/m ²)
Water	997.2	4180	0.6096	0.0009632
ZnO	5600	495.2	13	–
Water + 1% ZnO	1043	3982.35	0.6450	0.001
Water + 1.5% ZnO	1066	3889.83	0.6526	0.0011
Water + 2% ZnO	1089	3801.23	0.6605	0.00106

Table 2,
Material Thermophysical characteristics.

Material	Density (Kg/m ³)	Thermal conductivity (W/m K)	Specific heat (J/Kg K)
Aluminium	2719	202.4	871
Steel	8030	16.27	502.48

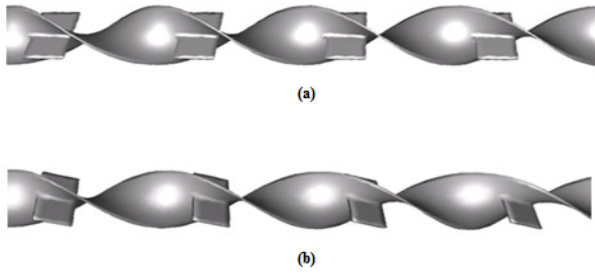


Fig. 1. (a) Baffle winged twist tape with baffle inclination angle ($\beta= 0^\circ$) (b) Baffle winged twist tape with baffle inclination angle ($\beta= 30^\circ$).

2.2. Nanofluids Thermophysical Properties

Nanofluids thermophysical properties were utilized as a part of this research using equations below [15]:

$$(\rho C p)_{nf} = (1 - \phi)(\rho C p)_f + \phi(\rho C p)_{np} \quad \dots(1)$$

$$\rho_{nf} = (1 - \phi)\rho_f + \phi\rho_{np} \quad \dots(2)$$

Where

$(\rho C p)_f$ and $(\rho C p)_{np}$ are heat capacity of the base liquid and the nanoparticles, respectively.

ρ_f and ρ_{np} are the densities of the base liquid and the nanoparticles, ϕ nanoparticle volume fraction

The effective thermal conductivity estimated using correlations below [15]:

$$K_{Static} = K_f \left[\frac{(K_{np} + 2K_f) - 2\phi(K_f - K_{np})}{(K_{np} + 2K_f) + \phi(K_f + K_{np})} \right] \quad \dots(3)$$

$$K_{Brownian} = 5 \times 10^4 \rho_f C p_f \phi \beta \sqrt{\frac{KT}{2\rho_{np} R_{np}}} f(T, \phi) \quad \dots(4)$$

$$K_{eff} = K_{Static} + K_{Brownian} \quad \dots(5)$$

Where

$\beta = 9.881(100\phi)^{-0.9446}$ for ZnO nanoparticle
k=Boltzmann constant

$$f(\phi, T) = (2.8217 \times 10^{-2} \phi + 3.917 \times 10^{-3}) \left(\frac{T}{T_0} \right) + (-3.669 \times 10^{-2} \phi - 3.391123 \times 10^{-3})$$

The effective viscosity estimated using the correlation below [16]:

$$\mu_{eff} = \frac{\mu_f}{(1 - 34.87 \times \phi^{1.03} \times (dp/df)^{-0.3})} \quad \dots(6)$$

$$df = \left[\frac{6M}{N \pi \rho_{fo}} \right] \quad \dots(7)$$

Where ρ_{fo} is the density of the base fluid at temperature $T_o=293$ K.

M is the molecular mass of base fluid.

N is the Avogadro number.

3. Data Structures and Numerical Analysis

3.1. Geometry Grid Creation

The geometry of baffle winged twist tape as exhibited in Figure 2 was generated by GAMBIT which exported to ANSYS-FLUENT 16 for simulation. This geometry model consists of a plain tube with length of 1800mm and 25.54 mm diameter. Plain twist tape with various ratio of twisting was created by twisting consistently piece of width equal to 25.54 mm which utilized by alternative turns edge of 360° for a length of 75, 100, and 125mm to produce the following twist ratios 2.93, 3.91 and 4.89. Though, the baffle winged twist tape geometry of with ratio of twisting ($y=2.93$) produced by using Cuboids of 25.54 mm width in the broad at a twist angle of 360° and 75 mm length.

The desired volume formed for simulation produced by subtract the baffle winged twist tape shape from the plain tube shape and the obtained model exported to the ANSYS-FLUENT 16 for meshing and simulation. Edge meshing is utilized using specific intervals, while the front surface was meshed by tetrahedral and pave mesh method, then the meshed surface swept through whole volume utilizing T grids form. The boundary conditions of the desired model including; model walls, inlet, outlet, and type of liquid (water) were characterized for CFD simulation.

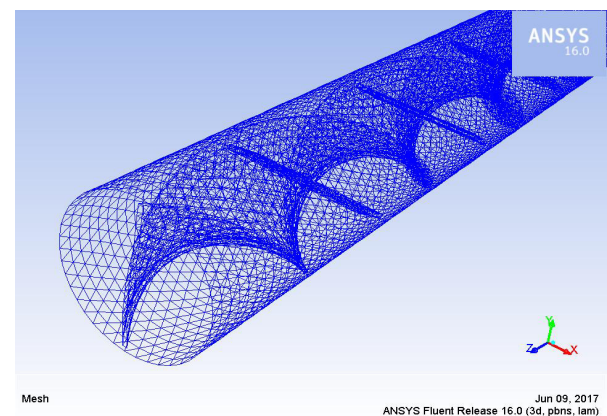


Fig. 2. Baffle winged twist tape grids with angle of inclination ($\beta= 30^\circ$).

3.2. Mathematical Model

3.2.1. Hypothesis

The suspension nanoparticles in water assumed as single phase fluid under thermal equilibrium. This assumption will precisely define the nanofluid behaviour in engineering cases. The case scrutinized for steady state and laminar flow conditions in three dimension using governing equations with numerical values illustrated in Table 3.

3.2.2 Equation of Mass Conservation.

$$\frac{\partial \rho}{\partial t} + \nabla \cdot (\rho \vec{v}) = S_m \quad \dots(8)$$

3.2.3 Equation of momentum Conservation

$$\rho \frac{\partial \vec{v}}{\partial t} + \rho (\vec{v} \cdot \nabla) \vec{v} = -\nabla p + \rho \vec{g} + \nabla \cdot \tau_{ij} + \vec{F} \quad \dots(9)$$

3.2.4 Equation of Energy Conservation.

$$\rho \frac{\partial}{\partial t} (\rho E) + \nabla \cdot \{ \vec{u} (\rho E + p) \} = S_h + \nabla \cdot \{ K_{eff} \nabla T - \sum h_i (\tau_{eff} \cdot \vec{v}) \} \quad \dots(10)$$

Table 3,
Numerical values used for simulation.

Reynolds Number (Re)	Heat flux (W/m ²)
240	782.92
350	1565.85
475	2348.78
600	3131.71
710	3914.63
840	4697.56
950	5480.5
1075	6263.42
1200	7046.35
2100	7829.27

4. Result and Discussion

4.1. Model Validation and Grid Independence Test

The independence of grid was investigated to evaluate mesh sizes influence on the recreated results about; five mesh work volumes were taken into account (401226, 532338, 656404, 727890

and 838278) for Re = 2000 which gives different values of Nusselt number with percentage deviation up to 0.3%. Subsequently, mesh work volume domain of 656404 was performed for plain tube and water as test fluid validates the model versus literature Stephan correlations [17]. Figures 3 and 4 demonstrate the variety of Nusselt number and friction coefficient with Reynolds number. Evidently, the results sensibly concurred well with these correlations.

4.2. Influence of Twist Ratio

Varieties of Nusselt and friction coefficients versus Reynolds number with plain twisted tape existence of are demonstrated in Figures 5 and 6. It's clearly noted that Nusselt and friction coefficients for minimum twist ratios were greater than those obtained from maximum ratio (y). This implied that the minimum twist ratio prompts greater tangential combination between the tube wall and swirl streams.

4.3. Influence of Tape Configuration

Variety of Nusselt and the friction coefficients versus Reynolds number with plain twist tape (y = 2.93) and baffle winged twist tape that has similar twist ratio (y=2.93, 3.91 and 4.89) and baffle inclination angles ($\beta = 0^\circ, -30^\circ$ and 30°) is appeared in Figures 7 and 8. It's discovered that the friction coefficient and Nusselt number for a tube with baffle winged twisted tape (y= 2.93) and baffle inclination angle ($\beta = -30^\circ$) was greater than the other twisted tapes. The baffle winged twist tape promote an extra liquid turbulences close to tube wall and vortices beyond the baffle winged shape which destructed the thermal boundary layers and generating supercar stream mixing between the liquid and heating surface

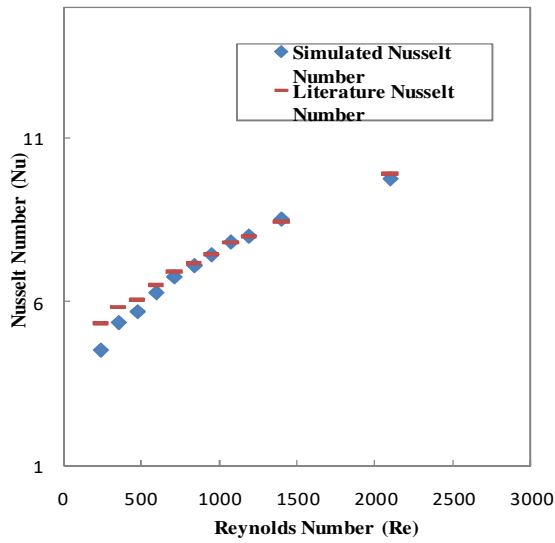


Fig. 3. Numerical Nusselt Number vs literature correlations for Plain tube.

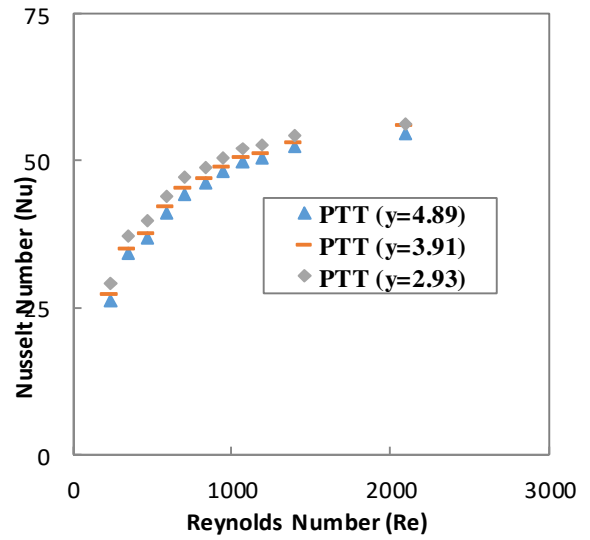


Fig. 5. The Influence of twist ratio on Nusselt Numbers.

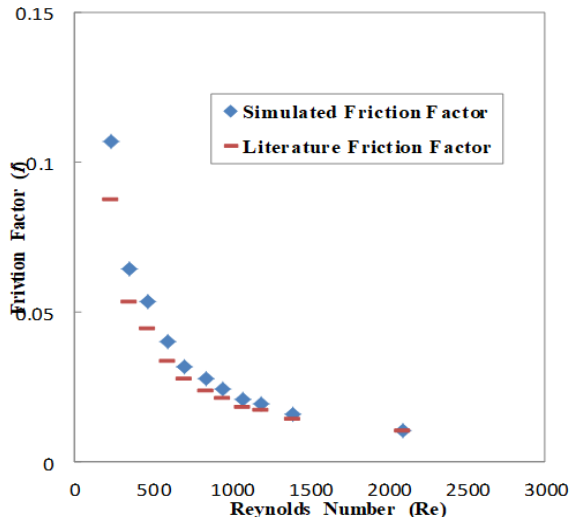


Fig. 4. Numerical Friction factor vs literature correlations for Plain tube.

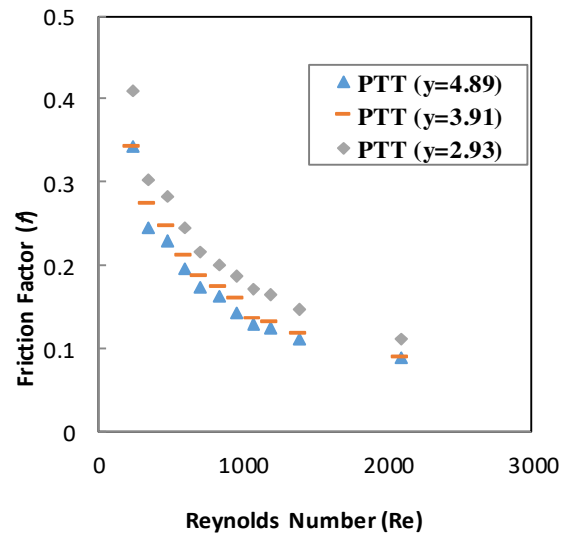


Fig. 6. The Influence of twist ratio on friction factor.

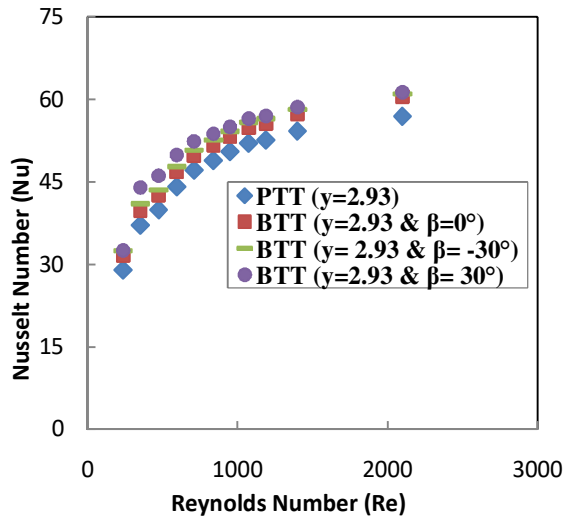


Fig. 7. The Influence of tape configuration on Nusselt number.

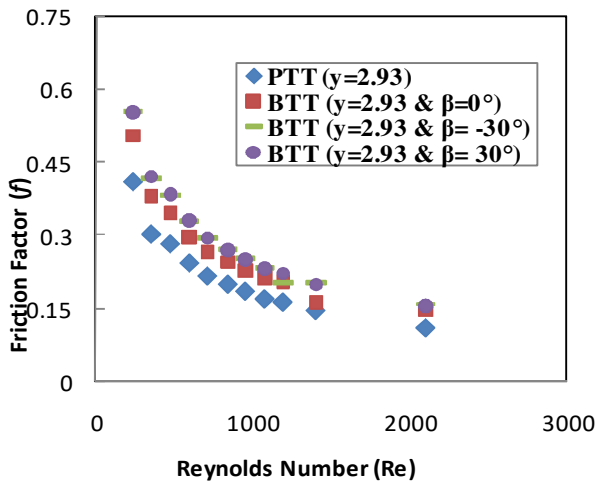


Fig. 8. The Influence of tape configuration on friction factor.

4.4. Influence of Tape Configuration with Nanofluids

The impact of Baffle winged tape with ratio of twisting $\gamma=2.93$ and baffle inclination angle ($\beta= -30^\circ$) with various volume fraction of ZnO nanofluid on Nusselt number and friction coefficient are illustrated in Figures 9 and 10. It is plainly noted from Figure 8 that the Nusselt number well improved with increments of nanoparticles concentration. This implies that the nanoparticles concentration enhanced the random movement of nanoparticles which improves fluid

flow thermal dispersion as well and vortices behind the baffle winged configuration. Figure 9 demonstrates the friction coefficient variation with the Reynolds number for various nanoparticles concentration. It's unmistakably noticed that the surface shear stress raised with the nanoparticles concentration expansion.

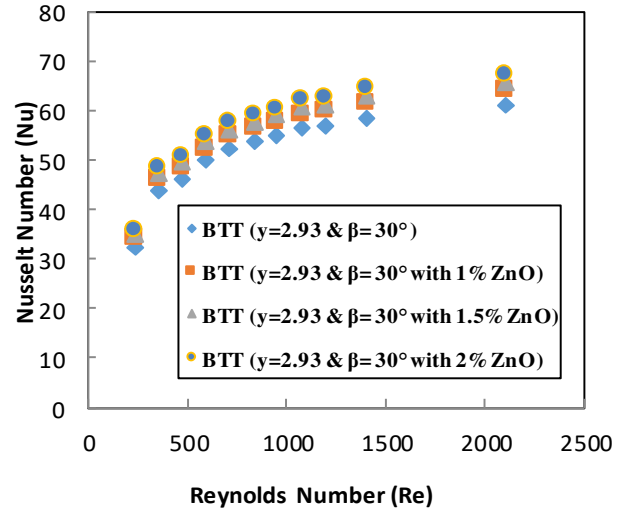


Fig. 9. The Influence of tape configuration with Nanofluid concentration on Nusselt number.

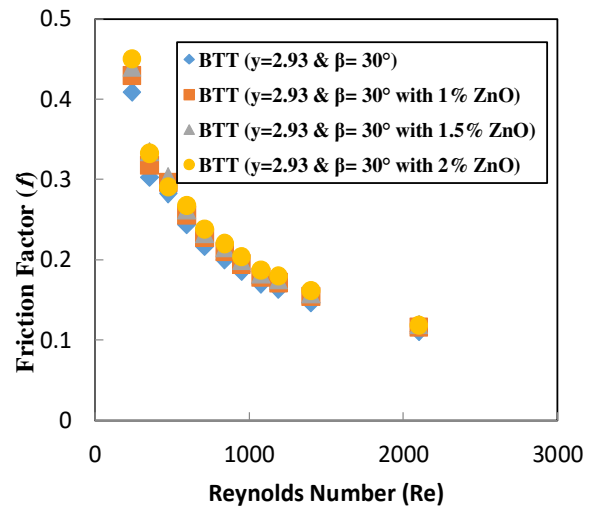


Fig. 10. The Influence of tape configuration with Nanofluid concentration on friction factor.

5. Conclusion

Numerical simulations for rate of heat transfer in a tube with classical and baffle winged tapes as well 1-2% volume fraction of ZnO nanofluid was completed utilizing by ANSYS-FLUENT version 16. The results obtained were matched with literature correlations for validation with the inconsistency up to $\pm 10\%$ for friction characteristics and $\pm 8\%$ for the Nusselt number. The results demonstrate that the Nusselt number expanded with the expansion of nanoparticles concentration, Reynolds number and twist ration as well baffle inclination angles diminishes. Likewise, the tape with $y=2.93$ and baffle inclination angles ($\beta= -30$) donated more prevailing than those of ($\beta= 0^\circ, 30^\circ$) for various Reynolds number. In addition, the tape with $y=2.93$ and baffle inclination angles ($\beta= -30$) combined with 2% ZnO nanofluid offers almost 10% improvements in Nusselt number values with considerable increments in friction coefficient than those obtained by classical tape.

Nomenclature

C_p	Fluid Heat Capacity, Joule/kg.K
dp	Size of Nanoparticle , nm
E	Energy, Joule
F	Force, Newton
f	Friction factor
g	Acceleration of gravity, m/s^2
k_{eff}	Thermal conductivity (Effective), Watt/m.K
m	mass flow, kg/sec
Re	Reynolds numbe, dimensionless
Nu	Nusselt number, dimensionless
p	Pressure, N/m ²
S_m	Mass accumulation, Kg
S_h	Energy accumulation, J
T	Temperature. K.
v	Velocity, m/sec
y	Ratio of twisting, dimensionless

Greek Letters

ρ	Density Kg/m ³
τ_{eff}	Shear stress, Newton/m ² .

Acknowledgment

We wish to specially acknowledge the assistance offered by the University of Baghdad

AL Khwarizmi College of Engineering for carrying our this investigation

6. References

- [1] M. Chandrasekar, S. Suresh, A.C. Bose, "Experimental studies on heat transfer and friction factor characteristics of Al₂O₃/water nanofluid in a circular pipe under laminar flow with wire coil inserts", *Experimental Thermal and Fluid Scienc* , vol. 34, Issue 2, pp. 122–130, 2010.
- [2] L.S. Sundar, K.V. Sharma, "Turbulent heat transfer and friction factor of Al₂O₃ nanofluid in circular tube with twisted tape inserts", *International Journal of Heat and Mass Transfer*, vol. 53, Issues 7–8, pp. 1409–1416, 2010.
- [3] S. Eiamsa-ard, P. Promvong, "Performance assessment in a heat exchanger tube with alternate clockwise and counter-clockwise twisted-tape inserts", *International Journal of Heat and Mass Transfer*, vol. 53, Issues 7–8, pp. 1364–1372, 2010.
- [4] P. Seemawute, S. Eiamsa-ard, "Thermohydraulics of turbulent flow through a round tube by a peripherally cut twisted tape with an alternate axis", *International Communications in Heat and Mass Transfer*, vol.37, Issue 6, pp. 652–659, 2010.
- [5] S. Eiamsa-ard, K. Wongcharee, P. Eiamsa-ard, C. Thianpong, "Heat transfer enhancement in a tube using delta- winglet twisted tape inserts", *Applied Thermal Engineering*, vol. 30, Issue 4, pp. 310–318, 2010.
- [6] P.K. Nagarajan, Y. Mukkamala, P. Sivashanmugam, "Studies on heat transfer and friction factor characteristics of turbulent flow through a micro-finned tube fitted with left-right inserts", *Applied Thermal Engineering*, vol. 30, Issue 13, pp. 1666–1672, 2010.
- [7] S. Eiamsa-ard, P. Promvong, "Thermal characteristics in round tube fitted with serrated twisted tape", *Applied Thermal Engineering*, vol. 30, Issue 13, pp. 1673–1682, 2010.
- [8] S. Eiamsa-ard, P. Seemawute, K. Wongcharee, "Influences of peripherally-cut twisted tape insert on heat transfer and thermal performance characteristics in laminar and turbulent tube flows", *Experimental Thermal and Fluid Science*, vol. 34, Issue 6, pp. 711–719, 2010.

- [9] S. Eiamsa-ard, K. Wongcharee, P. Eiamsa-ard, C. Thianpong, "Thermohydraulic investigation of turbulent flow through a round tube equipped with twisted tapes consisting of centre wings and alternate-axes", *Experimental Thermal and Fluid Science*, vol. 34, Issue 8, pp. 1151–1161, 2010.
- [10] S. Eiamsa-ard, C. Thianpong, P. Eiamsa-ard, P. Promvonge, "Thermal characteristics in a heat exchanger tube fitted with dual twisted tape elements in tandem", *International Communications in Heat and Mass Transfer*, vol. 37, Issue 1, pp. 39–46, 2010.
- [11] K. Wongcharee and S. Eiamsa-ard, "Friction and heat transfer characteristics of laminar swirl flow through a round tube inserted with alternate clockwise and counter-clockwise twisted-tapes", *International Communication in Heat and Mass Transfer*, vol. 38, Issue 3, pp. 348–352, 2011.
- [12] G. Pathipakka and P. Sivashanmugam, "Heat transfer behavior of nanofluids in a uniformly heated circular tube fitted with helical inserts in laminar flow", *Superlattices and Microstructure*, vol. 47, Issue 2, pp. 349–360, 2010.
- [13] S. D. Salman, A. A. H. Kadhum, M. S. Takriff, A. B. Mohamad, "CFD Simulation of Heat Transfer and Friction Factor Augmentation in a Circular Tube Fitted with Elliptic-Cut Twisted Tape Inserts", *Mathematical Problems in Engineering*, V. 2013, Article ID 163839, 7 pages, 2013.
- [14] S. D. Salman, A. A. H. Kadhum, M. S. Takriff, A. B. Mohamad, "Numerical Investigation of Heat transfer and friction factor characteristics in a circular tube fitted with V-cut twisted tape inserts", *The Scientific World Journal*, vol. 2013, Article ID 492762, 8 pages, 2013.
- [15] S. D. Salman, A. A. H. Kadhum, M. S. Takriff, A. B. Mohamad, "Heat transfer enhancement of laminar flow in a tube using Swirl / vortex Generator", *Australian Journal of Basic and Applied Sciences*, 8(19) Special 2014, Pages: 299-304
- [16] R.S. Vajjha, D.K. Das, "Experimental determination of thermal conductivity of three nanofluids and development of new correlations", *International Journal of Heat and Mass Transfer*, vol. 52, Issues 21–22, pp. 4675–4682, 2009.
- [17] M. Corcione, "Heat transfer features of buoyancy-driven nanofluids inside rectangular enclosures differentially heated at the side walls", *International Journal of Thermal Sciences*, vol. 49, Issue 9, pp. 1536–1546, 2010.
- [18] K. Stephan, and P. Preußer, "Wärmeübergang und maximale Wärmestromdichte beim Behältersieden binärer und ternärer Flüssigkeitsgemische", *Chemie Ingenieur Technik*, vol. 51, Issue 1, pp. 37, 1979.

تحسين الانتقال الحراري للموائع النانوية في أنبوب دائري مجهز بصفحة ملتوية ذات الأجنحة لتوليد الدوامات

سامي داود سلمان* رمزي عطا عبد الصاب**
 *قسم الهندسة الكيميائية الأحيائية/ كلية الهندسة الخوارزمي/ جامعة بغداد/ العراق
 *البريد الإلكتروني: sami.albayati@gmail.com
 **البريد الإلكتروني: ramzi_eng_1981@yahoo.com

الخلاصة

يقدم هذا البحث دراسة عددية عن التبادل الحراري ومعاملات الاحتكاك لتدفق المائع النانوي من الزنك والماء في أنبوب دائري مزود بمولد دوامة باستخدام ديناميك الموائع الحاسوبي. وقد استخدمت أشكال مختلفة من مولد الدوامات التي لها الخصائص الآتية: الصفحة الملتوية الكلاسيكية، الصفحة الملتوية ذات الأجنحة وبنسبة التواء ($y = 2.93, 3.91 \text{ and } 4.89$)، وبزاوية ميل للجناح ($30^\circ, -30^\circ, 0^\circ = \beta$) مع الجسيمات النانوية كأوكسيد الزنك وبتركيز حجمي يصل إلى (1%, 1.5, 2%) للمحاكاة. وقد أظهرت النتائج أن معاملات الحرارة والاحتكاك التي أجريت لهذين الشكلين من مولد الدوامات قد ازدادت بزيادة عدد رينولدز، ونقصان نسبة التواء الصفحة وزوايا ميل الجناح للصفحة، كما أظهرت النتائج أن معدل انتقال الحرارة قد ازداد بزيادة تركيز الجسيمات النانوية لأوكسيد الزنك. علاوة على ذلك، فإن الحد الأقصى لمعدل انتقال الحرارة مع زيادة ملحوظة في معامل الاحتكاك تم الحصول عليها الصفحة الملتوية ذات الأجنحة وبنسبة التواء ($y=2.93$) وبزاوية ميل تصل إلى ($30^\circ = \beta$) مع تركيز حجمي لأوكسيد الزنك النانوي يصل إلى 2% .